24. Olds, R. H., H. H. Reamer, B. H. Sage, and W. N. Lacey, *loc. cit.*, **41**, 475 (1949).
24a. Olds, R. H., B. F. Sage, and W. N. Lacey, *Ind. Eng. Chem.*, **38**, 301 (1946).
25. Onnes, H. Kamerlingh, *Commun. Phys. Lab. Univ. Leiden*, 11, Suppl. 23, 115 (1912).
25a. Organick, E. I., and W. R. Studhalter, *Chem. Eng. Progr.*, **44**, 847 (1948).
26. Prengle, H. W., L. R. Greenhaus, and Robert York, Jr., *Chem. Eng. Progr.*, **44**, 863 (1948).
27. Reamer, H. H., B. H. Sage, and W. N. Lacey, *Ind. Eng. Chem.*, **42**, 140 (1950).
28. *Ibid.*, **43**, 976 (1951).
29. Riedel, L., *Chem. Ing. Tech.*, **26**, 83 (1954).
30. "Refrigerating Data Book," 5 ed., Am. Soc. Refrigerating Engrs., New York (1942).
30a. Reid, R. C., and J. M. Smith, *loc. cit.*, **47**, 415 (1951).
31. Rynning, D. F., and C. O. Hurd, *Trans. Am. Inst. Chem. Engrs.*, **41**, 265 (1945).
32. Sage, B. H., and W. N. Lacey, *Ind. Eng. Chem.*, **32**, 992 (1940).
33. Sage, B. H., H. M. Lavender, and W. N. Lacey, *loc. cit.*, p. 743.
34. Sage, B. H., B. L. Hicks, and W. N. Lacey, *loc. cit.*, p. 1085.
35. Sage, B. H., H. H. Reamer, R. H. Olds, and W. N. Lacey, *loc. cit.*, **34**, 1108 (1942).
35a. Smith, J. M., *loc. cit.*, **44**, 521 (1948).
36. Streans, W. V., and E. J. George, *loc. cit.*, **35**, 602 (1943).
37. Stuart, E. B., K. T. Yu, and J. Coull, *Chem. Eng. Progr.*, **46**, 311 (1950).
38. Su, G. J., *Ind. Eng. Chem.*, **38**, 803 (1946).
39. van der Waals, J. D., "Die Continuität des gasförmigen und flüssigen Zustandes," Part II, Barth, Leipzig (1900).
40. Watson, K. M., *Ind. Eng. Chem.*, **35**, 398 (1943).
41. ———, and R. L. Smith, *Natl. Petroleum News* (July, 1936).
42. York, Robert, Jr., and E. R. White, Jr., *Trans. Am. Inst. Chem. Engrs.*, **40**, 227 (1944).

Presented at A.I.Ch.E. Detroit meeting

Turbulent Exchange of Mass and Momentum with a Boundary

THOMAS J. HANRATTY

University of Illinois, Urbana, Illinois

Visual observations by Fage and Townend of the behavior of a turbulent-flow stream near a boundary and experimental data by Lin, Moulton, and Putnam of concentration profiles near a boundary contradict the commonly held concept of the "laminar sublayer." A model developed by Higbie and Danckwerts which is consistent with the visual observations of Fage and Townend is used to describe the exchange of mass and heat between a turbulent fluid and a solid surface. It is postulated that masses of fluid are continuously moving to and from the wall. The exchange process then depends on the average contact time of these fluid masses with the wall.

The agreement of the concentration profile predicted on the basis of the proposed model with experimental mass transfer data where the exchange process is rate controlling lends support to the usefulness of the model. No equivalent data are available for velocity profiles. Velocity data represent a condition where the transport process within the fluid is playing an important role; however, in the immediate vicinity of the wall the proposed model might serve as a rough approximation of the profile. Such an approximation is made in this paper, and the agreement obtained is much better than should be expected.

That rates of momentum, heat, and mass transfer in a turbulent field are very much smaller in the vicinity of a surface than in the main body of a fluid has been recognized for a long time. In order to explain this phenomenon it has been postulated that there exists a thin nonturbulent layer of fluid adjacent to the wall. In this "laminar sublayer" momentum, heat, and mass are transported by random motion of the molecules rather than motion of macroscopic masses. As would be predicted by such a model, velocity-profile data extrapolate to a linear relationship between the velocity and distance in the vicinity of the wall. If, as is commonly assumed, the edge of the laminar sublayer is at the point where the velocity data deviate from linearity, its thickness may be calculated from the following empirical equation:

$$\frac{\delta_b}{d} = \frac{5}{Re}\sqrt{\frac{8}{f}} \qquad (1)$$

Fage and Townend (*1*) studied the behavior of fluid in the immediate vicinity of the wall by examining under the ultramicroscope the motion of dust particles in turbulently flowing water. The conditions of their experiments were such that the laminar-sublayer thickness as calculated by Equation (1) was about 0.03 in. Their experiments gave no evidence of the existence of a region possessing rectilinear motion. The following is a description of the flow very near the boundary given by Fage and Townend:

> With this magnification particles with a distance of 0.001 inch (0.0023*s*) from the surface were in focus. The view obtained showed a large number of particles moving in sinuous paths, and a few very slow particles which in the absence of a hairline in the eyepiece appeared to be moving in rectilinear paths. ... The slowest particles seen were therefore moving with a mean velocity of about 0.006 feet per second, and since the gradient $\partial(V/V_0)/\partial(n/s)$ at the surface was roughly 14, the distance of these particles from the surface was of the order of 1/40,000 inch. Attention could therefore be confined to the motion of particles at this distance from the boundary.
>
> It was first thought that these particles were moving in rectilinear paths, but it was noticed that their axial motions were frequently jerky (u, comparable with V, see later), and that sometimes they almost came to rest. A hairline was then inserted in the eyepiece of the microscope, and it subsequently appeared that all such particles moving near the hairline usually crossed and recrossed it several times. A considerable time was spent in observing these particles and the impression formed was that no particle was ever seen about which it could be said with conviction that its motion was rectilinear. In addition to these very slowly moving particles other faster particles could be observed at the same time on account of the finite thickness of fluid (0.001 inch) within the focus of the microscope. It occasionally happened that a group of

these particles made unusually large lateral excursions, and it was always observed that on these occasions the slowly moving particles would appear to shift laterally to other paths slightly removed from their previous ones. Sometimes two or more slowly moving particles, often widely separated, were observed to shift in step, and the whole appearance suggested that the violent motion in the faster moving fluid dragged the whole surface layer bodily sideways. It should follow that smaller lateral motions would also drag the surface layer sideways, but might do so to an extent too small to be observed, with the result that the flow during the intervals between these excursions would appear to be in rectilinear motion. It should also follow that below the critical speed, where no fluctuations in the motion were observed, the flow at the surface should be rectilinear. In turbulent flow v (velocity perpendicular to the boundary) is small but presumably finite near the boundary (except of course at the boundary), and the jerkiness of the axial motion due to the large fluctuations in u will be associated with the combined effect of very small changes in v and the large velocity gradient $(\partial U/\partial y)$ at the boundary.

Further evidence that in turbulent flow the fluid near the surface moves in relatively large masses was obtained during the experiments with the rotating objective now to be described.

Another contradiction of the commonly accepted concept of the laminar sublayer is reflected in a recent correlation by Lin, Moulton, and Putnam (*2*) of mass transfer data and of concentration profiles near the surface of concentration-polarized electrodes. The authors carried out experiments on the deposition of cadmium metal from cadmium sulfate solution onto a thin layer of fresh mercury supported on a smooth silver plate. The concentration distribution near the surface of the electrode was measured by means of light interference with a Mach-Zehnder type of interferometer. Measurements were carried out in a rectangular chamber under conditions such that the Reynolds number varied from 4,000 to 12,400. The Schmidt number was 900. Owing to the high Schmidt number the concentration of cadmium ions was essentially constant throughout the fluid and dropped from its main-stream value to zero at the wall within a space of less than 1 mm. The concentration profile was thus greatly dependent on conditions in the region described by Equation (1). The authors, finding it impossible to explain these measurements on the basis of a sublayer in laminar motion, assumed that turbulence existed in the laminar sublayer in which the eddy diffusion coefficient could be described approximately by the expression

$$\frac{\epsilon}{\mu} = \left(\frac{y^+}{14.5}\right)^3 \qquad (2)$$

Likewise in the correlation of mass transfer data over a wide range of Schmidt numbers Lin, Moulton, and Putnam (*2*), as well as Deissler (*3*), had to introduce turbulence into the laminar sublayer.

Visual observations of fluid behavior near a boundary and experimental data on rates of turbulent mass transfer and on concentration profiles, therefore, indicate either that the laminar sublayer is much thinner than has commonly been assumed or that it is nonexistent. If the first alternative be true, change of temperature, concentration, and velocity through it would be small and the sublayer would be unimportant as a transfer resistance.

In either case it appears as if it might be profitable to examine other models for explaining the turbulent exchange of heat, mass, and momentum with a solid surface or for describing the resistance to transfer in the region commonly ascribed to the laminar sublayer.

One such model which is consistent with the visual observation of Fage and Townend has been formulated by Danckwerts (*4*). It was first proposed by Higbie (*5*) to explain mass transfer in two-phase systems. According to this theory, the fluid in the immediate vicinity of the wall is not a continuous laminar layer but is discontinuous. Masses of fluid are pictured as moving to and from the wall, causing a continual change of the fluid in contact with the wall. The exchange of heat, mass, and momentum with the wall may then be visualized as occurring in the following manner. A mass of fluid comes in contact with the wall and its surface layer immediately assumes an equilibrium condition with the wall (same temperature, equilibrium concentration, zero velocity). Exchange of momentum, heat, and mass with the wall occurs. Just as with the unsteady heating or cooling of a block of metal, the rate of exchange between this fluid mass and the wall decreases with time. Eventually the mass of fluid is replaced and the whole process repeated. The contact time of these masses of fluid with the wall will vary. The smaller the average contact time of all masses of fluid coming in contact with the wall, the larger will be the measured exchange rate with the wall.

This paper has been written to show how such a model might be used to describe the measured concentration profiles of Lin, Moulton, and Putnam. It will also be shown that measured velocity profiles are not contradictory to the model. However, much more stringent assumptions must be made in the treatment of the velocity-profile data.

DISCONTINUOUS-FILM MODEL

Mathematical Formulation

Mathematical formulation of the discontinuous-film model will be accomplished by first considering the history of the surface layers of a fluid mass which comes in contact with the wall and then averaging the effect of all masses which will come in contact with the wall to calculate the exchange rate between the fluid and the surface.

If there is very little motion in surface layers of the fluid contacting the wall, then mass will be transferred through these layers by molecular diffusion and Fick's law will be applicable:

$$\frac{\partial C}{\partial \theta} = D\,\frac{\partial^2 C}{\partial y^2} \qquad (3)$$

For the data of Lin, Moulton, and Putnam the Schmidt number was high. Momentum is therefore transported much more rapidly than mass and the foregoing assumption is probably valid.

At high Schmidt numbers the concentration changes from the midstream value to an equilibrium value with the wall in a very short distance. For the experiments of Lin, Moulton, and Putnam, this was less than 1 mm. Therefore it will be assumed that the concentration of diffusing substance in a fluid mass approaching the wall will be uniform and equal to the midstream concentration. If the contact time is small enough, then the extent of the fluid mass in the y direction will not be important. Solutions for a semiinfinite medium may be used. With the following boundary conditions assumed

$$y = 0 \qquad C = C_W$$

$$y = \infty \qquad C = C_L$$

$$\theta = 0 \qquad C = C_L$$

Equation (3) may be solved for the concentration distribution and the rate of mass transfer (*6*):

$$\left(\frac{C - C_W}{C_L - C_W}\right) = \text{erf}\left(\frac{y}{2\sqrt{D\theta}}\right) \qquad (4)$$

$$(N_A) = (C_L - C_W)\sqrt{\frac{D}{\pi\theta}} \qquad (5)$$

Equations (4) and (5) give the concentration distribution and the instantaneous rate of mass transfer for a fluid mass which has been in contact with the wall for a time θ. For fluid masses having total contact lifetimes with the wall equal to θ_c, the probability for a contact time between θ and $\theta + d\theta$ is

$$\psi(\theta)\, d\theta = \frac{d\theta}{\theta_c} \qquad (6)$$

If all fluid masses had a contact lifetime of θ_c, then the measured concentration profile and rate of mass transfer would be

$$\left(\frac{C - C_W}{C_L - C_W}\right)_{\theta_c} = \int_0^{\theta_c} \text{erf}\left(\frac{y}{2\sqrt{D\theta}}\right)\frac{d\theta}{\theta_c} \qquad (7)$$

$$(N_A)_{\theta_c} = \int_0^{\theta_c} (C_L - C_W)\sqrt{\frac{D}{\pi\theta}}\frac{d\theta}{\theta_c}$$

$$= 2(C_L - C_W)\sqrt{\frac{D}{\pi\theta_c}} \qquad (8)$$

Actually, however, there will be a variation in the contact lifetime which must be taken into account. If the probability that a fluid mass possesses a lifetime between θ_c and $\theta_c + d\theta_c$ be defined as $\phi \, d\theta_c$, Equations (7) and (8) may be summed to give the actual measured average concentration distribution and transfer rate.

$$\frac{C - C_W}{C_L - C_W} \qquad (9)$$

$$= \int_0^{\infty} \phi(\theta_c)\left[\frac{1}{\theta_c}\int_0^{\theta_c} \text{erf}\left(\frac{y}{2\sqrt{D\theta}}\right)d\theta\right]d\theta_c$$

$$N_A = \frac{2(C_L - C_W)}{\sqrt{\pi}}\int_0^{\infty} \phi(\theta_c)\sqrt{\frac{D}{\theta_c}}\, d\theta_c \qquad (10)$$

A mass transfer coefficient may be defined in the following manner:

$$K = \frac{N_A}{C_L - C_W}$$

$$= \frac{2}{\sqrt{\pi}}\int_0^{\infty} \phi(\theta_c)\sqrt{\frac{D}{\theta_c}}\, d\theta_c \qquad (11)$$

Application to Measured Concentration Profiles

Use of Equations (9), (10), and (11) depends upon the evaluation of the probability function, $\phi(\theta_c)$, which has been assumed to have the form

$$\phi(\theta_c) = Ae^{-(\theta_c/\tau)^n} \qquad (12)$$

where A and τ are constants. The constant A may be evaluated in terms of τ from the relation

$$\int_0^{\infty} \phi(\theta_c)\, d\theta_c = 1 \qquad (13)$$

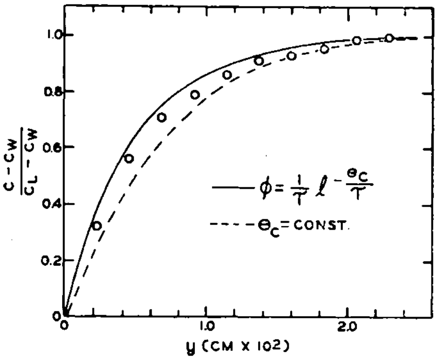

Fig. 1. Comparison of theory with measured concentration profiles.

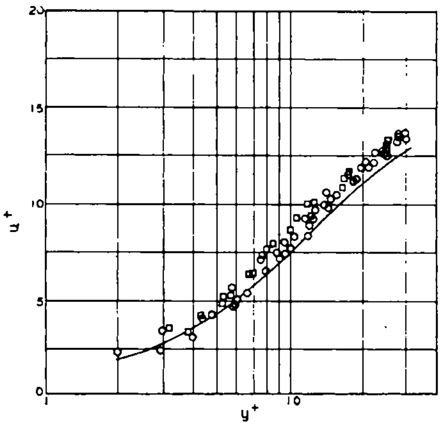

Fig. 2. Comparison of theory with measured velocity profiles.

The constant τ may be evaluated from experimental measurements of the mass transfer coefficient K. Table 1 presents the final form of a number of assumed probability functions for the age of the fluid masses. Form 1 represents the case in which the contact times of the fluid masses coming to the wall are of such a small range that their effect can be calculated by considering all these masses

TABLE 1. PROBABILITY FUNCTIONS REPRESENTING THE DISTRIBUTION OF EDDY AGES

Probability function	From Equation (26)	From Equation (21)	
1. θ_c = constant		$K = 2\sqrt{\frac{D}{\theta_c\pi}}$	$\theta_c = \frac{4D}{\pi K^2}$
2. $Ae^{-\theta_c/\tau}$	$A = \frac{1}{\tau}$	$K = \sqrt{\frac{D}{\tau}}$	$\tau = \frac{D}{K^2}$
3. $Ae^{-(\theta_c/\tau)^2}$	$A = \frac{2}{\sqrt{\pi}\,\tau}$	$K = \frac{\Gamma(1/4)}{\pi}\sqrt{\frac{D}{\tau}}$	$\tau = \frac{D}{K^2}\left[\frac{\Gamma(1/4)}{\pi}\right]^2$
4. $Ae^{-(\theta_c/\tau)^3}$	$A = \frac{3}{\tau\Gamma(1/3)}$	$K = \frac{\Gamma(1/6)}{\Gamma(1/3)}\sqrt{\frac{D}{\pi\tau}}$	$\tau = \frac{D}{\pi K^2}\left[\frac{\Gamma(1/6)}{\Gamma(1/3)}\right]^2$
5. $Ae^{-(\theta_c/\tau)^4}$	$A = \frac{4}{\tau\Gamma(1/4)}$	$K = \frac{\Gamma(1/8)}{\Gamma(1/4)}\sqrt{\frac{D}{\pi\tau}}$	$\tau = \frac{D}{\pi K^2}\left[\frac{\Gamma(1/8)}{\Gamma(1/4)}\right]^2$

TABLE 2. EFFECT OF ASSUMED EDDY AGE PROBABILITY FUNCTION UPON CALCULATION OF $(C - C_W)/(C_L - C_W)$

Measured $(C - C_W)/(C_L - C_W) = 0.59$ (*1*) $y = 0.50 \times 10^{-2}$ cm.

Probability function	Calculated $\frac{C - C_W}{C_L - C_W}$
Constant Age	0.50
$Ae^{-\theta_c/\tau}$	0.64
$Ae^{-(\theta_c/\tau)^2}$	0.66
$Ae^{-(\theta_c/\tau)^3}$	0.66
$Ae^{-(\theta_c/\tau)^4}$	0.67

to have the same θ_c. For this case the concentration profile may be calculated by Equation (7). The contact time θ_c may be evaluated from data on K by the equation presented in Table 1.

Equation (9) was used to calculate the concentration profile for test 87 of Lin et al. Data for K presented by Deissler (*3*) were used. The calculations and experimental measurements are presented in Figure 1. Only the probability functions represented by forms 1 and 2 of Table 1 were used in the graph. The particular probability function used did not appear greatly to affect the calculated profile. This is illustrated in Table 2 where calculated values of $(C - C_W)/(C_L - C_W)$ at $y = 0.50 \times 10^{-2}$ cm. are presented for different assumed-probability functions.

The agreement between the predicted and measured values, as presented in Figure 1, indicates that the discontinuous-film model supplies a satisfactory representation of these data. The agreement, in fact, is quite gratifying, as no arbitrary constants were used in the calculation. The profiles were predicted entirely from experimental values of K. This, of course, does not prove that the discontinuous-film model is a description of actuality. It shows only that it is a model which gives a better description than the laminar sublayer of the data of Lin, Moulton, and Putnam (*2*) and which is not in contradiction to the visual observations of Fage and Townend (*1*).

Since one of the arguments in support of the laminar-sublayer concept is the prediction of velocity data, it would be desirable to examine the reasonableness of the discontinuous-film model in light of these data. Such an examination presents difficulties which cannot be entirely overcome, but after some simplifying assumptions are made it may be attempted. The results of the comparison will be presented not to support the discontinuous-film model but only to show that velocity-profile data are not in contradiction to it.

COMPARISON OF VELOCITY DATA

The prediction of velocity data in the immediate vicinity of the wall on the basis of the discontinuous-film model is handicapped for the following reasons.

1. Under the conditions under which all the velocity data have been obtained, the rate of transport of momentum to the vicinity of the wall is important. The exchange of momentum with the wall is not controlling. The velocity does not increase to the free-stream velocity in the region commonly ascribed to the laminar sublayer. It is therefore difficult to ascribe an average velocity to the fluid masses arriving at the wall.

2. The average velocity measured at any point in a turbulent field represents contributions of eddies of different frequencies. The probability of any individual eddy having a particular velocity will depend on its frequency. Consequently, the velocity of a mass of fluid arriving at the wall will probably be dependent upon the amount of time during which the mass will be in contact with the wall. This presents a degree of complication over the description of the mass and heat transfer processes, as to describe the phenomenon accurately a double probability function would be needed, expressing the probability that a mass of fluid will have a velocity between $u_L + du_L$ and a contact time between θ_c and $\theta_c + d\theta_c$.

3. The model proposes only to describe the exchange of momentum with the wall. The diffusion of momentum to the wall is probably governed by a more complex process than is represented by the model. Consequently predicted velocity profiles in the vicinity of the wall should be regarded only as a first approximation.

In order to circumvent these difficulties the following assumptions will be made.

1. The wall exchange process on the average can be represented by the motion of masses of fluid possessing a fixed velocity u_L and a fixed wall-contact time θ_c.

2. The transport of momentum within any one of these masses can be represented by the equation

$$\frac{\partial u}{\partial \theta} = \frac{\mu}{\rho}\left(\frac{\partial^2 u}{\partial y^2}\right) \tag{14}$$

By use of the boundary conditions

$$y = 0 \qquad u = 0$$

$$y = \infty \qquad u = u_L$$

$$\theta = 0 \qquad u = u_L$$

Equation (14) may be solved to give the velocity distribution and the instantaneous rate of momentum transfer with the wall for a fluid mass which has been in contact with the wall for a time θ (*6*).

$$u = u_L \operatorname{erf}\left(\frac{y}{2\sqrt{\frac{\mu}{\rho}\theta}}\right) \tag{15}$$

$$\tau_0 g_c = \rho u_L \sqrt{\frac{\mu}{\rho \pi \theta}} \tag{16}$$

Now the probability for a fluid mass to have been in contact with the wall for a time between θ and $\theta + d\theta$ is

$$\psi(\theta)\, d\theta = \frac{d\theta}{\theta_c} \tag{6}$$

Averaging the effect of all masses in contact with the wall gives the predicted measured velocity distribution and the predicted measured rate of momentum transfer to the wall

$$u = \frac{u_L}{\theta_c}\int_0^{\theta_c} \operatorname{erf}\left(\frac{y}{2\sqrt{\frac{\mu}{\rho}\theta}}\right) d\theta \tag{17}$$

$$\tau_0 g_c = \int_0^{\theta_c} \rho u_L \sqrt{\frac{\mu}{\rho\pi\theta}}\frac{d\theta}{\theta_c}$$

$$= 2\rho u_L \sqrt{\frac{\mu}{\rho\pi\theta_c}} \tag{18}$$

By use of Equation (18), the expression for the velocity distribution, Equation (17), may be put into a form which can be compared with experimental data:

$$\frac{u}{\sqrt{\tau_0/\rho}} = \frac{u_L}{\sqrt{\tau_0/\rho}} \cdot \int_0^1 \operatorname{erf}\left(\frac{y^+\sqrt{\tau_0/\rho}\,\sqrt{\pi}}{u_L 4\sqrt{\theta/\theta_c}}\right) d\left(\frac{\theta}{\theta_c}\right) \tag{19}$$

Equation (19) gives a first approximation of the velocity profile in the vicinity of the wall based on the discontinuous-film model using the assumptions outlined in this section. Essentially it embodies one arbitrary constant, $u_L/\sqrt{\tau_0/\rho}$.

In order to carry out a comparison with experimental data it has been assumed that

$$\frac{u_L}{\sqrt{\tau_0/\rho}} = 13.5 \tag{20}$$

This expression arises from a consideration of measurements of velocity profiles (*2* and *3*). When these data are plotted on semilog paper two distinct regions are noted. The major portion of the data fall on a straight line. However, very close to the wall there is a break from this linearity. The portion of the field represented by the straight line has usually been referred to as the *turbulent core* and the nonlinear region has been referred to as the *buffer layer* and the *laminar sublayer*. It seems reasonable to assume that the latter region is the one over which the influence of the wall is felt. Therefore the fluid masses moving against the wall have been assumed to possess a velocity equal to that at the break point. This break point occurs at $y^+ = 30$ and the value of $u/\sqrt{\tau_0/\rho}$ represented by Equation (20).

Substituting Equation (20) into Equation (19) results in the following relation between $u^+ = u/\sqrt{\tau_0/\rho}$ and y^+.

$$\frac{u}{\sqrt{\tau_0/\rho}} = 13.5 \cdot \int_0^1 \operatorname{erf}\left(\frac{y^+\sqrt{\pi}}{13.5 \times 4 \times \sqrt{\theta/\theta_c}}\right) d\left(\frac{\theta}{\theta_c}\right) \tag{21}$$

Owing to the boundary conditions selected, $u = u_L$ at $y = \infty$, one would expect the foregoing expression to hold only for values of y^+ much less than 30.

Equation (21) has been plotted in Figure 2 along with experimental data presented by Deissler (*3*). The agreement is far better than would be suspected. Actually even better agreement would have been obtained by use of a larger value of $u_L/\sqrt{\tau_0/\rho}$ in Equation (19).

NOTATION

- C = concentration
- C_L = concentration of diffusing material in fluid mass before contact with the wall
- C_W = concentration at the wall
- d = pipe diameter
- D = molecular diffusion coefficient
- f = Fanning friction factor = $4\tau_0/(\frac{1}{2}\rho U_0^2)$
- K = mass transfer coefficient = $N_A/(C_L - C_W)$
- N_A = rate of mass transfer per unit area
- Re = Reynolds number = $(dU_0\rho)/\mu$
- $2s$ = length of side of square pipe
- u, U = velocity in axial direction
- U_0 = average fluid velocity
- u_L = velocity in axial direction of fluid mass before contact with the wall
- u^+ = $u/\sqrt{(\tau_0 g_c)/\rho}$
- y = perpendicular distance from the wall
- y^+ = $y\sqrt{(\tau_0 g_c)/\rho}\;\rho/\mu$
- δ_b = thickness of laminar sublayer
- θ = time
- θ_c = total time for which a fluid mass had been in contact with the wall
- μ = fluid viscosity
- ρ = fluid density
- τ = constant appearing in distribution function
- τ_0 = shear stress at the wall

LITERATURE CITED

1. Fage, A., and H. C. H. Townend, *Proc. Roy. Soc. London*, **135A**, 656 (1932).
2. Lin, C. S., R. W. Moulton, and G. L. Putnam, *Ind. Eng. Chem.*, **45**, 636, 640 (1953).
3. Deissler, R. G., *Natl. Advisory Comm. Aeronaut. Tech. Note* 3145 (May, 1954).
4. Danckwerts, P. V., *Ind. Eng. Chem.*, **43**, 1460 (1951).
5. Higbie, R., *Trans. Am. Inst. Chem. Eng.* vs. **31**, 65 (1935).
6. Carslaw, H. S., and J. C. Jaeger, "Conduction of Heat in Solids," Oxford University Press, London (1947).